Preprints of the 19th World Congress
The International Federation of Automatic Control
Cape Town, South Africa. August 24-29, 2014

An Online Estimation of Rotational Velocity of Flying Ball via Aerodynamics

Akira Nakashima * **Takeshi Okamoto** * **Yoshikazu Hayakawa** *

* *Mechanical Science and Engineering, Graduate School of Engineering, Nagoya University, Furo-cho, Chikusa-ku, Nagoya, Japan (e-mail: a_nakashima@nuem.nagoya-u.ac.jp)*

Abstract: We propose a novel estimation method of the rotational velocity of a flying ball as well as its position and translational velocity via aerodynamics model by measuring the ball trajectory using the middle speed cameras for table tennis system. The aerodynamics model is complex nonlinear and the measured data of the ball trajectory has quantization errors because the size of the ball is very small in the field of view of the middle speed cameras. Then, we consider the estimation by minimizing the *difference between the trajectories* which are measured by the cameras and numerically solved by integrating the aerodynamics model respectively. Since the difference is not analytical function, the minimization is solved by the downhill simplex method, where some modification is introduced for improving the converge speed. The effectiveness of the method is verified by numerical simulations.

Keywords: Optimal estimation, Estimation algorithms, State estimation, Robotics, Model-based recognition, Physical models, Table tennis system, Online estimation

1. INTRODUCTION

Dynamic manipulation is dexterous task of humans by utilizing dynamics of manipulated targets (Mason and Lynch (1993)). Ball sports are examples of the dynamic manipulation because there are intermittent interactions between balls and players or environments. Table tennis is a typical example since flying time of ball is very short, e.g. 550 [ms] because the ball speed is fast and the distance between players is close (usual speed is 5.0 [m/s] (Tamaki et al. (2004))). It is therefore essential to rapidly recognize the ball in the opponent's court and *predict the ball trajectory* in order to plan the racket motion at the time when a player hits the ball. Since these issues are very attractive and challenging, many researchers have studied and developed robots playing table tennis (Zhang et al. (2008)).

Models of ball motion including flying and rebounds on the table and racket are necessary for the prediction of the ball trajectory. The models have been dealt with by two methodologies, one of which is based on input-output black-box or grey-box models, e.g. Miyazaki et al. (2002); Matsushima et al. (2005), and the other of which is based on explicit physical models, e.g. Hashimoto et al. (1987); Anderson (1988); Zhang et al. (2010); Yang et al. (2010). In these studies, the *rotational velocity was not considered* although it effects on the ball trajectory when the ball is flying and rebounds. Especially in the case of table tennis, since the rotational velocity is very large (3000 [rpm]) and the ball's mass is very light (2.7 [g]), the spin effects are much bigger than the ones in other ball sports (Tamaki et al. (2004)).

We have developed a robotic table tennis system as shown in based on physical models of ball where the effects of the rotational velocity are considered. The ball is shot from the automatic ball catapult machine. The robotic table tennis system consists of the subtasks of 1) the ball recognition; 2) the ball trajectory prediction; 3) the racket motion determination; and 4) the motion planning for the racket motion. **1)** The ball recognition is the measurement of the position, translational/rotational velocities of a flying ping-pong ball, which is performed by an online-estimation method (Liu et al. (2011, 2012)) using the *high-speed* vision cameras (1000fps) (Nakabo et al. (2000)). **2)** With the measured ball states, the ball trajectory is predicted to provide the ball's position and velocities at the hitting time using the aerodynamics model (Nonomura et al. (2010)) and rebound model of the table (Nakashima et al. (2010b)). **3)** The racket motion means the velocity and orientation at the predicted position and at the time of arrival of the ball. The racket motion is determined as to make the ball hit by the racket arrive to desired points in the opponent's court using the aerodynamics model and rebound model of the racket (Nakashima et al. (2011,

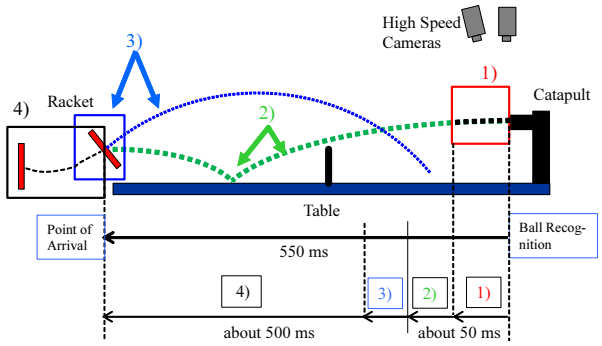

Fig. 1. Table Tennis System with High Speed Cameras.

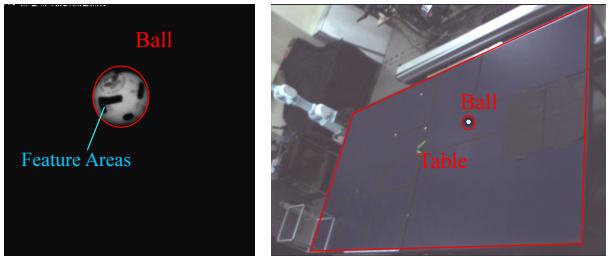

Fig. 2. Fields of view of High speed and Middle speed Cameras.

2012); Liu et al. (2013)). **4)** The robot is controlled along trajectory planned to the predicted hitting point at the time of arrival. These tasks are performed sequentially as shown in the lower of Fig. 1, where the subtasks 1) and 2) have to be terminated as fast as possible to assure time enough for the robot to move by the subtasks 3) and 4).

The left figure of Fig. 2 shows the field of view of the high speed camera, where the flying ball is measured. The *feature areas* on the ball is necessary for measuring the rotational velocity. Unfortunately, because the field of view of the high speed camera is *very small* (about 15 [cm] square) due to its high sampling rate, the cameras can only measure narrow areas around the ball catapult as the illustrated red square in Fig. 1. Then, it is impossible for the system to play with a human player. On the other hand, middle speed cameras (150fps) can measure area including whole table as shown in the right figure of Fig. 2. However, it is impossible to measure the feature areas on the ball since the ball is too small in the field of view of the middle speed camera. Furthermore, the sampling rate is not high enough to measure the high speed rotational velocity using the feature area.

Figure 3 shows some ball trajectories with different rotational velocities which are calculated by the aerodynamics model of the ball (Nonomura et al. (2010)). The red, green, blue and black lines represent the spins of top, back, left-side and right side respectively. The sold and dashed lines denote the different magnitudes of the rotational velocities, 100 and 300 [rad/s] respectively. It is found that the every trajectories are different from each other. This

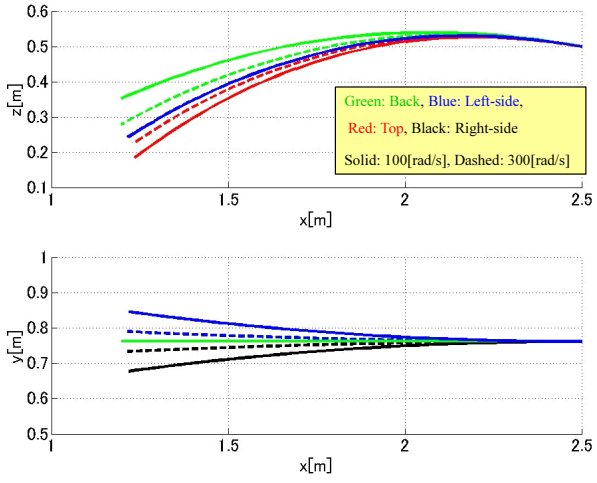

Fig. 3. Ball Trajectories with Different Rotational Velocities.

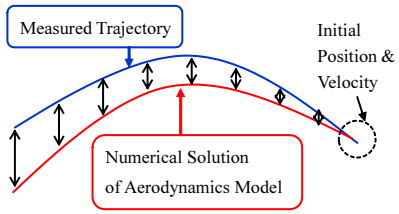

Fig. 4. Difference between Measured and Numerically Solved Trajectories of Ball.

imply that the rotational velocity can be estimated by the measured ball trajectory via the aerodynamics model.

Therefore, we propose a novel estimation method of the rotational velocity as well as the position and translational velocity via the aerodynamics model by measuring the ball trajectory using the middle speed cameras. Note that the table tennis system becomes new one where the subtask 1) in Fig. 1 is replaced to the proposed one. The aerodynamics model is complex nonlinear and the measured data of the ball trajectory has quantization errors because the size of the ball is very small in the field of view of the middle speed cameras. Then, as shown in Fig. 4, we consider the estimation by minimizing the *difference between the trajectories* which are measured by the cameras and numerically solved by integrating the aerodynamics model respectively. Since the difference is not analytical function, the minimization is solved by the downhill simplex method (Nelder and Mead (1965)), where some modification is introduced for improving the converge speed.

The robotic table tennis system is briefly explained in Section 2. The aerodynamics model is described in Section 3. The estimation method is proposed in Section 4. The method is verified by various cases of conditions of ball trajectories in numerical simulations in Section 5. Some conclusions and future work are shown in Section 6.

2. ROBOTIC TABLE TENNIS SYSTEM

2.1 Experimental System

Figure 5 illustrates our robotic table tennis system. The table is an international standard one with the sizes of 1.525(W)×0.760(H)×2.740(D) [m]. The ball is shot out from the automatic ball catapult, ROBO-PONG 2040 (SAN-EI Co.). The flying ball is measured by the two color middle-speed cameras (150fps) of the Radish System (Library, Co.). The reference frame Σ_B is set at the right corner of the robot's court. The racket is attached to the robot's tip and its board and rubber are Fukuhara-Ai Special and Bryce Speed FX (Butterfly, Ltd.). The distance from the center to the edge of the racket is about 75 [mm]. The PCs for the control and visual measurement are Dell Precision T5500 (CPU: Intel(R)Xeon E5503 2.66GHz, Memory: 2GB RAM) and Dell Precision T5300 (CPU: Intel(R)Xeon E5430 2.66GHz, Memory: 2GB RAM). The OS of the PCs are Windows XP Professional sp2 and the program language is C++. The measured position of the ball is transmitted to the PC for the control by the LAN with the sampling time $\Delta t = 1/150 \simeq 6.7$ [ms]. In the estimation method, the ball prediction and the

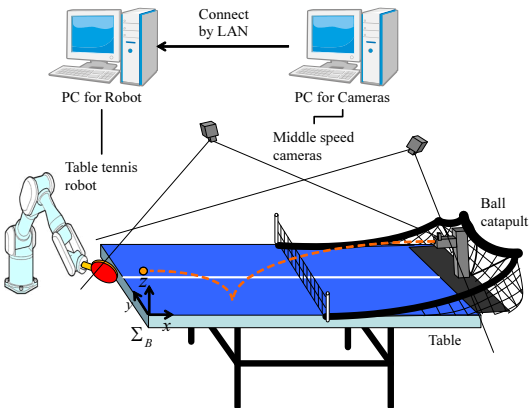

Fig. 5. Robotic Table Tennis System.

determination of the racket motion are performed in the PC for the control.

2.2 Scheme of Subtasks with Middle Speed Cameras

Figure 6 shows the scheme of hitting a flying ball. The subtasks 1)–4) have been already explained in Section 1. In the middle of the figure, the red, green and blue squares represent the time intervals where the subtasks 1), 2) and the set of 3), 4) are performed respectively. Note that the time intervals are overlapped in the interval $[t_1,\ t_2]$ while the intervals of the subtasks are completely separated in the previous system as shown in Fig. 1. This reason is explained as follows.

Since the estimation method is based on the difference between the measured and calculated trajectories, the accuracy of the result depends on the number of the data of the trajectory. As shown in latter, enough number is about 60 while it is 6 in the method using the high speed cameras. This number corresponds to the trajectory to the

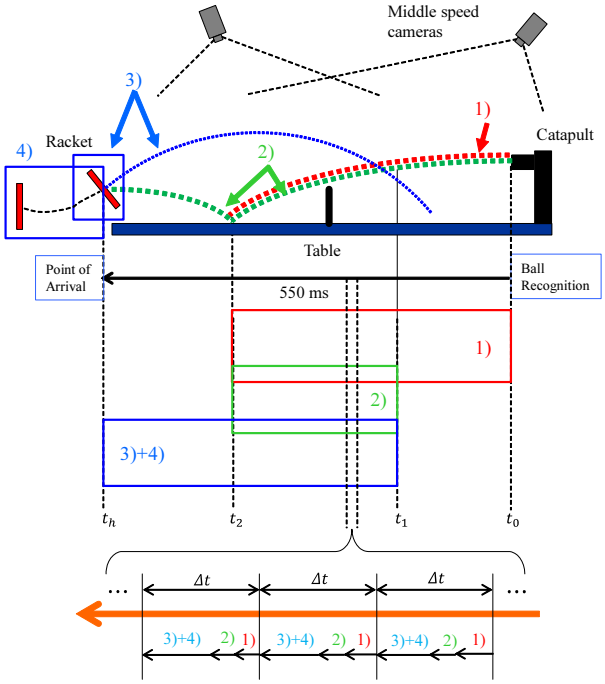

Fig. 6. Table Tennis System with Middle Speed Cameras.

position just before the rebound on the table. It is obvious that the time of the rebound, $t = t_2$ is too late to start the subtasks 2) to 4), i.e. the prediction and the robot control. Therefore, the subtasks 2) and the pair of 3) and 4) has to be started before the time of the rebound, i.e. has to be started at $t = t_1 < t_2$.

In the interval $[t_1,\ t_2]$, it is ideal that the sequential process consisting of the subtasks 1) to 4) is executed at every sampled times as illustrated in the lowest of Fig. 6, which represents some sampling time intervals in the interal $[t_1,\ t_2]$. Therefore, the processing time of the estimation method in the subtask 1) has to be *short* enough for all the subtasks to be terminated during the sampling time Δt. Furthermore, the method has to be *accurate* enough for the *predicted position of arrival* in the subtask 2) using the estimated value in the subtask 1) to be close to the real position such that the racket can hit the ball. Intuitively, the error of the predicted position has to be smaller than the radius of the racket.

3. AERODYNAMICS MODEL

Define the ball position as $\boldsymbol{p} = [p_x\ p_y\ p_z]^{\mathrm{T}} \in \mathbb{R}^3$ and the rotational velocity as $\boldsymbol{\omega} = [\omega_x\ \omega_y\ \omega_z]^{\mathrm{T}} \in \mathbb{R}^3$. The rotational velocity $\boldsymbol{\omega}$ is assumed to be constant. Then, the aerodynamics model of the ball is given by (Nonomura et al. (2010))

$$m\ddot{\boldsymbol{p}} = -m\boldsymbol{g} - \frac{1}{2}\rho S_b C_D(\dot{\boldsymbol{p}}, \boldsymbol{\omega})\|\dot{\boldsymbol{p}}\|\dot{\boldsymbol{p}} + \rho V_b C_M(\dot{\boldsymbol{p}}, \boldsymbol{\omega})\boldsymbol{\omega} \times \dot{\boldsymbol{p}}, \tag{1}$$

where $S_b := \pi r^2$ is the ball cross section area, $V_b := \frac{4}{3}\pi r^3$ is the ball volume, $r = 0.02$ [m] is the ball radius, $m = 0.0027$ [kg] is the ball mass, $\rho = 1.184$ [kg/m^3] is the air density and and $\boldsymbol{g} := [0\ 0\ g]^{\mathrm{T}}$ with $g = 9.8$ [m/s^2] is the acceleration of gravity. In the right hand of (1), the second and third terms represent the drag and lift effects with their coefficients C_D and C_M as shown in Fig. 7.

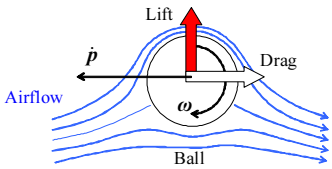

Fig. 7. Drad and Lift Forces of Rotated Flying Ball.

The coefficients depend on the directions of the rotational velocity $\boldsymbol{\omega}$, i.e. the top, back and side spins, which are described in Fig. 8. In the left figure, $\dot{\boldsymbol{p}}_{xy} := [\dot{p}_x\ \dot{p}_y\ 0] \in \mathbb{R}^3$ represents the x and y components of the ball velocity in

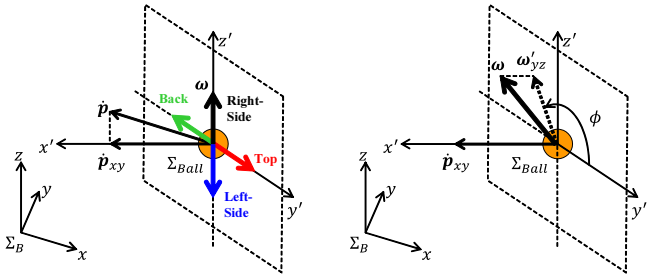

Fig. 8. Definitions of Top, Back and Side Spins.

the reference frame Σ_B. The frame Σ_{Ball} is defined such that the x'- and z'-axes are along the direction of $\dot{\boldsymbol{p}}_{xy}$ and the z-axis of Σ_B. The orientation of Σ_{Ball} relative to Σ_B is represented by the rotational matrix

$$\boldsymbol{R}_{Ball}(\psi) := \begin{bmatrix} \cos\psi & -\sin\psi & 0 \\ \sin\psi & \cos\psi & 0 \\ 0 & 0 & 1 \end{bmatrix}, \tag{2}$$

where ψ is the angle between the x- and x'- axes of the frames defined by

$$\cos\psi := \frac{\dot{p}_x}{\sqrt{\dot{p}_x^2 + \dot{p}_y^2}}, \quad \cos\psi := \frac{\dot{p}_y}{\sqrt{\dot{p}_x^2 + \dot{p}_y^2}}.$$

The top and back spins are defined as the axes along the positive and negative directions of the y'-axis respectively. The side spin is defined as the positive and negative directions of the z'-axis. The coefficients are changed in terms of the types of the spin, i.e. the axes directions as follows:

$$\begin{aligned} C_D &= a_D + b_D \cos\phi, \\ C_M &= a_M + b_M \cos\phi, \end{aligned} \tag{3}$$

where $a_D = 0.505$, $b_D = 0.065$ and $a_M = 0.094$, $b_M = -0.026$. As shown in the right figure of Fig. 8, ϕ is defined as the angle of the rotational velocity $\boldsymbol{\omega}'_{yz} \in \mathbb{R}^3$, which is obtained by projecting $\boldsymbol{\omega}' := \boldsymbol{R}_{Ball}^{\mathrm{T}}(\psi)\boldsymbol{\omega}$ onto the (y', z')-plane:

$$\boldsymbol{\omega}'_{yz} = [0,\ \omega'_y,\ \omega'_z]^{\mathrm{T}} := [0,\ \omega_y \cos\psi - \omega_x \sin\psi,\ \omega_z]^{\mathrm{T}}. \tag{4}$$

Note that $\phi = 0, \pm 90, 180$ [deg] represent the spins of the top, side and back respectively. By using (2) and (4), the angle ϕ is represented in terms of the ball translational/rotational velocities $(\dot{p}_x, \dot{p}_y)$ and (ω_x, ω_y) by

$$\cos\phi = \frac{\omega'_y}{\sqrt{\omega'^2_y + \omega'^2_z}} = \frac{\dot{p}_x\omega_y - \dot{p}_y\omega_x}{\sqrt{(\dot{p}_x\omega_y - \dot{p}_y\omega_x)^2 + (\dot{p}_x^2 + \dot{p}_y^2)\omega_z^2}}. \tag{5}$$

4. ESTIMATION METHOD

4.1 Overview of Estimation

Since the rotational velocity $\boldsymbol{\omega}$ is estimated based on the difference between the measured and numerically solved trajectories as shown in Fig. 4, the initial position and velocity, $\boldsymbol{p}_{ini}$ and $\dot{\boldsymbol{p}}_{ini}$ are necessary for the integration of the aerodynamics model. Although the initial values can be obtained by the measured data, these also has to be estimated to reduce the measuring error of the cameras. Therefore, the estimation method is decomposed of two phases as shown in Fig. 9; the first estimation phase for the initial position $\boldsymbol{p}_{ini}$ and the second estimation phase for the rotational velocity $\boldsymbol{\omega}$ and the initial velocity $\dot{\boldsymbol{p}}_{ini}$. The first phase uses the data from the initial time step $k = 1$ $(t = t_0)$ to the current time step k. This estimation is performed at the sampled time steps iteratively until conditions of *phase termination* are satisfied. Then, the estimated initial position $\boldsymbol{p}^*_{ini}$ is obtained. After the first phase is terminated at a time step, e.g. $k = k_1$, the second phase is performed using the data from the initial time step $k = 1$ to current time step $k > k_1$ at the sampled time steps iteratively with the estimated initial position $\boldsymbol{p}^*_{ini}$ until a condition of phase termination is satisfied. Note that the phase termination means that the phases are terminated.

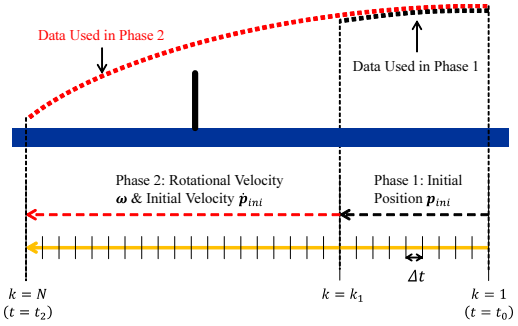

Fig. 9. Scheme of Estimation in Subtask 1).

4.2 Phase 1: Estimation of Initial Position

In the first phase, the ball trajectory is approximated as a quadratic polynomial with respect to time t as follows:

$$\bar{\boldsymbol{p}}(t_k; \boldsymbol{\theta}) = \boldsymbol{c}_2 t_k^2 + \boldsymbol{c}_1 t_k + \boldsymbol{c}_0 \tag{6}$$

where $\boldsymbol{\theta} := [\boldsymbol{c}_0^{\mathrm{T}}\ \boldsymbol{c}_1^{\mathrm{T}}\ \boldsymbol{c}_2^{\mathrm{T}}]^{\mathrm{T}} \in \mathbb{R}^9$ is the parametric vector and $\boldsymbol{c}_j := [c_{jx}\ c_{jy}\ c_{jz}]^{\mathrm{T}} \in \mathbb{R}^3$ $(j = 0, 1, 2)$ denotes the coefficients of the jth order term in the polynomial in the x-, y- and z-axes and $t_k := (k-1)\Delta t$ is the ith sampled time. The approximation is performed by solving the minimization problem with the following performance function at kth time step:

$$J_{1,k}(\boldsymbol{\theta}) := \sum_{i=1}^{k} ||\boldsymbol{p}_i - \bar{\boldsymbol{p}}(t_i; \boldsymbol{\theta})||^2, \tag{7}$$

where $\boldsymbol{p}_i$ is the measured ball position at the ith time step. Since the problem with (7) is quadratic with respect to the coefficients $\boldsymbol{\theta}$, it can be solved with the linear least-squares method. Define $\boldsymbol{\theta}^*$ as the optimized parametric vector. Then, the initial position $\boldsymbol{p}_{ini}$ is estimated as

$$\boldsymbol{p}^*_{ini} = \bar{\boldsymbol{p}}(0; \boldsymbol{\theta}^*) = \boldsymbol{c}_0^*. \tag{8}$$

This optimization is performed iteratively at the sampled times until the following conditions of the phase termination: (i) the difference between the optimized positions, i.e. $\|\bar{\boldsymbol{p}}(0; \boldsymbol{\theta}^*_k) - \bar{\boldsymbol{p}}(0; \boldsymbol{\theta}^*_{k-1})\|$ is smaller than a specified threshold; (ii) p_{x_k} is smaller than 1.37[m] which is the half length of the table.

4.3 Phase 2: Estimation of Initial Translational Velocity and Rotational Velocity

As mentioned in Section 1, the estimation of the rotational velocity $\boldsymbol{\omega}$ and the initial velocity $\dot{\boldsymbol{p}}_{ini}$ is performed based on the difference between the measured trajectory $\boldsymbol{p}_i$ and

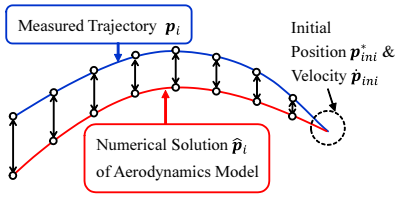

Fig. 10. Criterion in Phase 2: Difference between Measured and Numerically Solved Trajectories of Ball Using Initial Position Obtained in Phase 1.

the one $\hat{\boldsymbol{p}}_i$ solved by integrating the aerodynamics model (1) with the estimated initial position $\boldsymbol{p}^*_{ini}$ as illustrated in Fig. 10. The sequence of the numerically solved ball position $\hat{\boldsymbol{p}}_i$ $(i = 1, \cdots, k)$ is obtained with the Euler method as

$$\begin{aligned} \hat{\boldsymbol{p}}_{i+1} &= \hat{\boldsymbol{p}}_i + \hat{\boldsymbol{v}}_i \Delta t \\ \hat{\boldsymbol{v}}_{i+1} &= \hat{\boldsymbol{v}}_i + \boldsymbol{f}(\hat{\boldsymbol{v}}_i, \boldsymbol{\omega}) \Delta t \end{aligned} \tag{9}$$

where

$$\boldsymbol{f} := -\boldsymbol{g} - \frac{\rho S_b C_D(\hat{\boldsymbol{v}}_i, \boldsymbol{\omega})}{2m} \|\hat{\boldsymbol{v}}_i\| \hat{\boldsymbol{v}}_i + \frac{\rho V_b C_M(\hat{\boldsymbol{v}}_i, \boldsymbol{\omega})}{m} \boldsymbol{\omega} \times \hat{\boldsymbol{v}}_i,$$
$$\hat{\boldsymbol{p}}_1 := \boldsymbol{p}^*_{ini}, \quad \hat{\boldsymbol{v}}_1 := \dot{\boldsymbol{p}}_{ini}.$$

Since the lift effect is represented by the cross product of $\dot{\boldsymbol{p}}$ and $\boldsymbol{\omega}$, it is sufficient to consider the components of $\boldsymbol{\omega}$ perpendicular to $\dot{\boldsymbol{p}}$. Therefore, as an approximated situation, we introduce the following constraint for the rotational velocity $\boldsymbol{\omega}$:

$$[\dot{p}_{x_{ini}} \ \dot{p}_{y_{ini}} \ 0]^{\mathrm{T}} \boldsymbol{\omega} = 0, \tag{10}$$

where $\dot{p}_{x_{ini}}$ and $\dot{p}_{y_{ini}}$ are the components of the x- and y-axes of $\dot{\boldsymbol{p}}_{ini}$. The constraint (10) represents that the rotational velocity $\boldsymbol{\omega}$ is included in the (y', z') of Σ_{Ball} as shown in Fig. 8. The constraint (10) expresses the realistic situation where almost all the cases of balls hit by an usual racket are either the top, back or side spins. Therefore, the rotational velocity $\boldsymbol{\omega}$ is reduced to its y and z components in Σ_{Ball} defined as

$$\tilde{\boldsymbol{\omega}} := [\tilde{\omega}_y \ \tilde{\omega}_z]^{\mathrm{T}} \in \mathbb{R}^2 \tag{11}$$

which is translated to the rotational velocity $\boldsymbol{\omega}$ by the relationship:

$$\boldsymbol{\omega} = \boldsymbol{R}_{Ball}(\psi_{ini}) \begin{bmatrix} 0 \\ \tilde{\boldsymbol{\omega}} \end{bmatrix}, \tag{12}$$

where

$$\cos\psi_{ini} := \frac{\dot{p}_{x_{ini}}}{\sqrt{\dot{p}^2_{x_{ini}} + \dot{p}^2_{y_{ini}}}}, \quad \cos\psi_{ini} := \frac{\dot{p}_{y_{ini}}}{\sqrt{\dot{p}^2_{x_{ini}} + \dot{p}^2_{y_{ini}}}}.$$

Therefore, the objective variable in the optimization is defined as

$$\boldsymbol{q} := \begin{bmatrix} V\dot{\boldsymbol{p}}_{ini} \\ W\tilde{\boldsymbol{\omega}} \end{bmatrix} \in \mathbb{R}^5 \tag{13}$$

where W and V are the weight parameters for $\tilde{\boldsymbol{\omega}}$ and $\dot{\boldsymbol{p}}_{ini}$ and are set as $W = 5.0 \times 10^{-4}$ and $V = 2$ in this paper.

Therefore, we solve the minimization problem with the following performance function at the kth time step:

$$J_{2,k}(\boldsymbol{q}) = \sum_{i=1}^{k} \|\boldsymbol{p}_i - \hat{\boldsymbol{p}}_i(\boldsymbol{p}^*_{ini}, \boldsymbol{q})\|^2. \tag{14}$$

Define $\boldsymbol{q}^0_k$ and $\boldsymbol{q}^*_k$ as the initial and optimized values at kth time step. Then, the initial value $\boldsymbol{q}^0_k$ is set to the previous optimized value $\boldsymbol{q}^*_{k-1}$ as follows:

$$\boldsymbol{q}^0_k = \boldsymbol{q}^*_{k-1}, \quad \boldsymbol{q}^0_1 = \begin{bmatrix} V\dot{\boldsymbol{p}}^0_{ini} \\ W\tilde{\boldsymbol{\omega}}^0 \end{bmatrix} \tag{15}$$

where $\boldsymbol{q}^0_1$ is the first initial value. The initial value $\tilde{\boldsymbol{\omega}}^0$ is a specified values, e.g. $[145, 145]^{\mathrm{T}}$ [rad/s] and $\dot{\boldsymbol{p}}^0_{ini}$ is given by the time derivative of the estimated initial position in the first phase as follows:

$$\dot{\boldsymbol{p}}^0_{ini} = \frac{d}{dt}\boldsymbol{p}(t; \boldsymbol{\theta}^*)\Big|_{t=0} = \boldsymbol{c}^*_1. \tag{16}$$

This optimization is performed iteratively at the each sampled time step until the following condition of the phase termination: the ball height p_{z_k} is smaller than 0.05 [m] which means that the ball almost rebounds on the table. Since the performance function (14) is not an analytical one, we solve the problem with the downhill simplex method (Nelder and Mead (1965)). Its explanation, parameter setting and modification are omitted because of space limitation.

5. VERIFICATION OF ESTIMATION METHOD

The effectiveness of the estimation method is verified by numerical simulations. The measured data is produced by solving the aerodynamics model with white noise. The initial conditions of the data are set as $\boldsymbol{p}_{ini} = [2.5, 0.7625, 0.8]^{\mathrm{T}}$ [m] and $\dot{\boldsymbol{p}}_{ini} = [-5.43, 0.0, 0.8]^{\mathrm{T}}$ [m/s], which are referring to the values in the measurement of the situations where usual humans play table tennis. The rotational velocity $\boldsymbol{\omega}$ is set to $[0, \ \eta\cos\xi, \ \eta\sin\xi]^{\mathrm{T}}$ [rad/s], where $\eta = 50i, (i = 1, \cdots, 7)$ and $\xi = \frac{(j-1)\pi}{6}, (j = 1, \cdots, 12)$. The cases of $j = 1$, $j = 4, 10$ and $j = 7$ correspond to the top, side and back spins respectively. The total number of the data is 84. The termination threshold in the first phase is 1.0×10^{-6} [m].

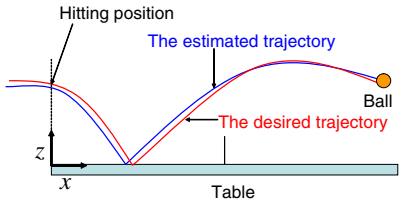

Fig. 11. Verification Criterion of Estimation.

The results of the estimation should be evaluated in the situation that the robot hits balls. Define the hitting times when the balls arrive at the side of the table near the robot, i.e. $p_x = 0$ as shown in Fig. 11. Then, in detail, the positions at the hitting times are compared which are obtained by integrating the aerodynamics model with the desired and estimated values of $\boldsymbol{p}_{ini}$, $\dot{\boldsymbol{p}}_{ini}$ and $\boldsymbol{\omega}$. The estimation is judged as successful when the error of the positions at the hitting time is smaller than 0.075 [m] of the racket radius and the error of the estimated and true rotational velocities is smaller than 100 [rad/s]. Note that the rebound phenomenon on the table is simulated by the rebound model proposed by Nakashima et al. (2010a).

All the estimation results of the second phase are shown in Fig. 12. The optimizations of the first phase are omitted because they are trivial. The histories of the errors with respect to the time step are plotted. The upper and lower figures represent the errors of the hitting position and rotational velocity respectively. The blue solid lines, black dotted lines and the red circles represent the errors, the thresholds and the errors at the terminated time step respectively. The rate of the success with all the trial data is 91.1%. It is found that almost all errors are close to the thresholds around the time step 40 ($t \simeq 0.27$ [s]) and are smaller than the thresholds around the time step 60 ($t \simeq 0.40$ [s]). The time when the errors are close to the thresholds is smaller than half of averaged flying time of the balls, 0.55 [s]. Then, it is possible for the prediction and the robot control to be started at this early time. The

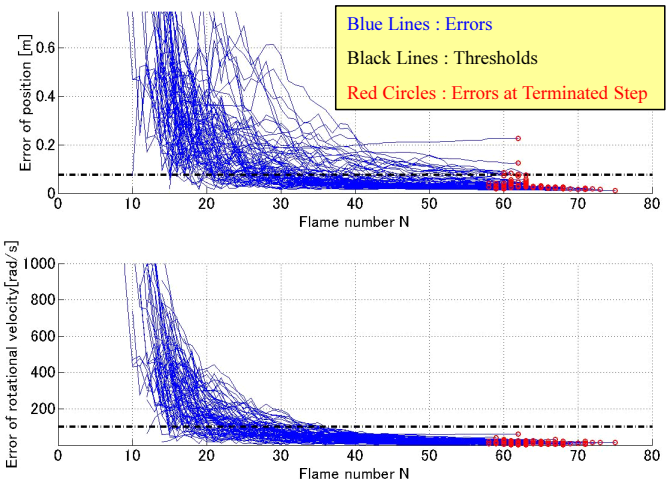

Fig. 12. Errors of Verifications of Hitting Point and Rotational Velocity.

results guarantee that the proposed method is useful for the table tennis robot system.

6. CONCLUSIONS

We have proposed a novel estimation method of the rotational velocity of a flying ball as well as its position and translational velocity via aerodynamics model by measuring the ball trajectory using the middle speed cameras for table tennis system. As the criterion in the estimation, the difference between the trajectories is used which are measured by the cameras and numerically solved by integrating the aerodynamics model respectively. The downhill simplex method is utilized for the optimization with some modification for improving the converge speed. The effectiveness of the method was verified by numerical simulations.

Combining the trajectory prediction and the robot control with the proposed method is one of our future work. And the application of it to the real system where the robot plays with a human is another future work.

REFERENCES

Anderson, R.L. (1988). *A robot ping-pong player: experiment in real-time intelligent control.* MIT Press, Cambridge, MA, USA.

Hashimoto, H., Ozaki, F., Asano, K., and Osuka, K. (1987). Development of a pingpong robot system using 7 degrees of freedom direct drive arm. In *Proc. Int. Conf. IECON*, 608–615.

Liu, C., Hayakawa, Y., and Nakashima, A. (2011). A registration algorithm for on-line measuring the rotational velocity of a table tennis ball. In *Proc. IEEE ROBIO*, 2270–2275.

Liu, C., Hayakawa, Y., and Nakashima, A. (2012). An on-line algorithm for measuring the translational and rotational velocities of a table tennis ball. *SICE JCMSI*, 5(4), 233 – 241.

Liu, C., Hayakawa, Y., and Nakashima, A. (2013). Racket control for a table tennis robot to return a ball. *SICE JCMSI*, 6(4), 259 – 266.

Mason, M. and Lynch, K. (1993). Dynamic manipulation. In *Proc. IEEE/RSJ IROS*, volume 1, 152–159.

Matsushima, M., Hashimoto, T., Takeuchi, M., and Miyazaki, F. (2005). A learning approach to robotic table tennis. *IEEE Trans. Robot.*, 21(4), 767 – 771.

Miyazaki, F., Takeuchi, M., Matsushima, M., Kusano, T., and Hashimoto, T. (2002). Realization of the table tennis task based on virtual targets. In *Proc. IEEE ICRA*.

Nakabo, Y., Ishikawa, M., Toyoda, H., and Mizuno, S. (2000). 1ms column parallel vision system and its application of high speed target tracking. In *Proc. IEEE Int. Conf. Robot. Automat.*, 650–655.

Nakashima, A., Nonomura, J., Chunfang, L., and Hayakawa, Y. (2012). Hitting back-spin balls by robotic table tennis system based on physical models of ball motion. In *Proc. IFAC SYROCO 2012*, 834–841.

Nakashima, A., Ogawa, Y., Chunfang, L., and Hayakawa, Y. (2011). Robotic table tennis based on physical models of aerodynamics and rebounds. In *Proc. IEEE ROBIO*, 2348–2354.

Nakashima, A., Ogawa, Y., Kobayashi, Y., and Hayakawa, Y. (2010a). Modeling of rebound phenomenon of a rigid ball with friction and elastic effects. In *Proc. IEEE Amer. Cont. Conf.*, 1410–1415.

Nakashima, A., Tsuda, Y., Liu, C., and Hayakawa, Y. (2010b). A real-time measuring method of translational/rotational velocities of a flying ball. In *Proc. 5th IFAC Sym. on Mech. Sys.*, 732–738.

Nelder, J.A. and Mead, R. (1965). A simplex method for function minimization. *The Computer Journal*, 7, 308–313.

Nonomura, J., Nakashima, A., and Hayakawa, Y. (2010). Analysis of effects of rebounds and aerodynamics for trajectory of table tennis ball. In *Proc. SICE Annual Conf.*, 1567 –1572.

Tamaki, T., Sugino, T., and Yamamoto, M. (2004). Measuring ball spin by image registration. In *Proc. 10th Frontiers of Computer Vision*, 269–274.

Yang, P., Xu, D., Wang, H., and Zhang, Z. (2010). Control system design for a 5-dof table tennis robot. In *11th Int. Conf. ICARCV*, 1731 –1735.

Zhang, Z., Xu, D., and Tan, M. (2010). Visual measurement and prediction of ball trajectory for table tennis robot. *IEEE Trans. Instru. Meas.*, 59(12), 3195 –3205.

Zhang, Z., Xu, D., and Yu, J. (2008). Research and latest development of ping-pong robot player. In *7th World Cong. Intel. Contr. Auto.*, 4881 –4886.